Clim Dyn
DOI 10.1007/s00382-009-0718-1

Climate entropy budget of the HadCM3 atmosphere–ocean general circulation model and of FAMOUS, its low-resolution version

Salvatore Pascale · Jonathan M. Gregory · Maarten Ambaum · Rémi Tailleux

Received: 6 August 2009 / Accepted: 27 November 2009

Abstract The entropy budget is calculated of the coupled atmosphere–ocean general circulation model HadCM3. Estimates of the different entropy sources and sinks of the climate system are obtained directly from the diabatic heating terms, and an approximate estimate of the planetary entropy production is also provided. The rate of material entropy production of the climate system is found to be $\sim$50 mW m^{-2} K^{-1}, a value intermediate in the range 30–70 mW m^{-2} K^{-1} previously reported from different models. The largest part of this is due to sensible and latent heat transport ($\sim$38 mW m^{-2} K^{-1}). Another 13 mW m^{-2} K^{-1} is due to dissipation of kinetic energy in the atmosphere by friction and Reynolds stresses. Numerical entropy production in the atmosphere dynamical core is found to be about 0.7 mW m^{-2} K^{-1}. The material entropy production within the ocean due to turbulent mixing is $\sim$1 mW m^{-2} K^{-1}, a very small contribution to the material entropy production of the climate system. The rate of change of entropy of the model climate system is about 1 mW m^{-2} K^{-1} or less, which is comparable with the typical size of the fluctuations of the entropy sources due to interannual variability, and a more accurate closure of the budget than achieved by previous analyses. Results are similar for FAMOUS, which has a lower spatial resolution but similar formulation to HadCM3, while more substantial differences are found with respect to other models, suggesting that the formulation of the model has an important influence on the climate entropy budget. Since this is the first diagnosis of the entropy budget in a climate model of the type and complexity used for projection of twenty-first century climate change, it would be valuable if similar analyses were carried out for other such models.

Keywords Entropy budget · General circulation models · Material entropy production

S. Pascale (✉) · J. M. Gregory · M. Ambaum · R. Tailleux
Department of Meteorology, University of Reading,
Earley Gate, Reading RG6 6BB, UK
e-mail: s.pascale@reading.ac.uk

J. M. Gregory
Met Office Hadley Centre, Exeter EX1 3PB, UK

1 Introduction

The climate is an important example of a *non-equilibrium steady state* system. The *non-equilibrium* nature of the climate system means that a variety of irreversible processes must be taking place continuously within it, whereas the *steady* characteristic implies that a time-independent balance must exist for some relevant physical quantities, for example energy, angular momentum and water. The physical quantity which is able to describe both the irreversibility (non-equilibrium) and the steadiness of the climate system at once (and of any non-equilibrium steady state system) is the *entropy production rate* of the system (Kondepudi and Prigogine 1998; DeGroot and Mazur 1984).

In contrast to energy fluxes, at the top of the atmosphere, in a steady state, the outgoing entropy flux exceeds the incoming: *entropy is produced*. The rate of entropy production of the system, due to irreversible processes, must be positive in order to satisfy the second law of thermodynamics. However, the rate of change of entropy must be zero if the system is in a steady state.

General circulation models (GCMs) are generally not designed to diagnose entropy, but at the moment there is

Published online: 16 December 2009

increasing interest in entropy production as a diagnostic tool for GCMs. This is motivated in part by the intriguing Maximum Entropy Production (MEP) conjecture (Paltridge 1975), for a general review see Martyushev and Seleznev (2006) or Kleidon and Lorenz (2005), and Kleidon (2009) for a view of all the variety of applications to the Earth system) and its possible applications for improving GCMs (Kunz et al. 2008). Moreover, entropy seems to have a role in the basic thermodynamics of the climate: for example Pauluis and Held (2002) showed that the efficiency of convection is reduced by the entropy production of non-viscous processes (such as water vapour diffusion). Furthermore, Johnson (1997) argued that spurious numerical entropy sources (of either sign—a negative source is a sink) can affect the simulated general circulation of the atmosphere; his example was the cold bias at high latitude and altitude found in many GCMs. Recently, Lucarini et al. (2009) used entropy production concepts and other thermodynamic quantities to study a solar constant variation hysteresis experiment.

Some previous entropy budgets have been published based on observational analyses, theoretical calculations and model simulations. Fraedrich and Lunkeit (2008) used a 25-year integration of the Planet Simulator, a model of intermediate complexity (Fraedrich et al. 2005). Goody (2000) diagnosed entropy terms from a six-year control run using the atmospheric component of Goddard Institute of Space Studies (GISS) model with sea-surface temperatures (SSTs) maintained at climatological temperatures and also gave some theoretical values for the most important material entropy production terms. Peixoto et al. (1991) also made some order-of-magnitude estimates on the basis of energy flux values of Peixoto and Oort (1984).

As noted in Fraedrich and Lunkeit (2008) entropy budgets of complex GCMs have not attracted much attention in the scientific literature. In this paper we present the first analysis of the entropy budget of a complex coupled atmosphere–ocean general circulation model (AOGCM). This is the type of model used for projection of anthropogenic climate change during the twenty-first century. It would be desirable if similar entropy budget diagnostics were calculated in other AOGCMs in order to enable comparisons.

The paper is organised in the following way. Section 2 describes the setup of runs being analysed. The entropy budget equations are outlined in Sect. 3 and the method used to diagnose the associated entropy sources is described. In Sect. 4, we consider the radiation and show an approximate method to calculate the irreversible entropy production and the net entropy flux at the top of the atmosphere. Section 5 discusses the atmospheric diabatic processes in HadCM3 due to the hydrological cycle and sensible heat. The meaning of the energy correction term in HadCM3 and the kinetic energy dissipation is outlined in Sect. 6, while in Sect. 7 the numerical entropy source of the HadCM3 dynamical core is analysed. Section 8 deals with the ocean component of the model and provides direct estimates of the rate of entropy production in the body of the ocean by turbulent mixing. Section 9 discusses the uncertainty in the material entropy production and compares different model values. The paper ends with a summary of the key results in Sect. 10.

2 Models and experiments

The AOGCM used in this paper is HadCM3 (Gordon et al. 2000; Pope et al. 2000) and its low resolution version, FAMOUS (Jones et al. 2005), of which we are using version FAMOUS-xdbua (Smith et al. 2008). HadCM3 has been widely used to simulate present day and future climate and compares well with other current AOGCMs of the Coupled Model Intercomparison Project (Reichler and Kim 2008).

HadCM3 and FAMOUS are configurations of the Met Office (UK) unified forecast and climate model. Apart from some minor differences the physics and the dynamics are the same. By virtue of the reduced horizontal and vertical resolution and increased timestep FAMOUS runs about ten times faster than HadCM3. This characteristic is particularly useful for long runs or large ensembles of integrations, for which HadCM3 is too expensive in terms of time and resources. However, the reduced resolution means inevitably that the climate in FAMOUS is somewhat less realistic, though still satisfactory for our investigative purposes.

The runs subjected to entropy budget analysis are 50-year runs with a pre-industrial CO_2 concentration.

2.1 The atmosphere

The atmosphere model of HadCM3 has a horizontal grid spacing of $2.5° \times 3.75°$ and 19 vertical levels. The timestep is 30 min. The horizontal atmospheric grid-spacing of FAMOUS is $5° \times 7.5°$, twice that used in HadCM3, and the vertical resolution is reduced to 11 levels. A timestep of 1 h is used.

The dynamic core is a split-explicit finite difference scheme (Cullen and Davies 1991). Each timestep consists of an adjustment step followed by a Heun advection step. The prognostic variables are the zonal and meridional wind component, $\mathbf{v} \equiv (u, v)$, the surface pressure p_*, the specific humidity q and the potential air temperature θ. At the end of every integration step a Fourier filter is applied to avoid the numerical need for a very short timestep. The advection should be a fully adiabatic process but the numerical scheme can introduce spurious numerically generated entropy sources/sinks (Egger 1999; Johnson 1997).

Hyper-diffusion (sixth-order in HadCM3, eighth in FAMOUS) is applied after the advection to the model prognostics. The temperature hyper-diffusion leads to a small local heating and the momentum hyper-diffusion to a dissipation of kinetic energy (Boville and Bretherton 2003).

The physical parametrisation schemes (see Sects. 5–8) include: (a) the radiation scheme (Edwards and Slingo 1996), (b) the convection scheme (Gregory and Rowntree 1990), (c) the large-scale cloud scheme (Smith 1990), (d) the large-scale precipitation scheme (Gregory 1995), (e) the boundary layer scheme (Smith 1990). At the end of every timestep an energy and mass correction is applied to impose conservation. The atmosphere model includes the surface model, over both land and ocean, which simulates surface fluxes of latent and sensible heat and momentum, i.e. windstress.

2.2 The ocean

The ocean component in HadCM3 is a 20 level version of the Cox (1984) model on a 1.25° × 1.25° latitude–longitude grid. In FAMOUS this resolution is reduced to 2.5° × 3.75° with the 20 vertical levels unchanged. A 1-h time step is used to integrate the model in HadCM3, 12 h in FAMOUS. The Boussinesq approximation is adopted, in which density differences are neglected except in the buoyancy term. The hydrostatic assumption is made in which local acceleration and other terms of equal order are eliminated from the equation of vertical motion. In order to suppress rapidly travelling external waves, the model has a flat rigid surface, which exerts a downward pressure in lieu of the weight of a variable sea level. The prognostic variables are sea-water potential temperature θ, salinity and horizontal velocity.

In the ocean shortwave radiation is partly absorbed at the surface (red component) and partly (blue component) selectively with depth using a double exponential decay. Within the ocean various parametrisation schemes are employed to represent small-scale turbulent mixing (see Sect. 8).

The atmospheric and ocean model are coupled once per day. The atmosphere model is run with fixed SSTs through the day and the various fluxes are accumulated after each atmospheric time step. At the end of the day these fluxes are passed to the ocean model which is then integrated forwards in time and supplies SSTs and sea-ice conditions back to the atmosphere.

3 The climate entropy budget

3.1 Planetary entropy production

The spatial domain of the climate system encompasses matter (i.e. the fluid which constitutes the atmosphere and the oceans, the solid Earth and the cryosphere), and radiation, which extends beyond the Earth system but which penetrates it and interacts with the matter. The major effect of this interaction is an energy gain or loss: the climate gains $\dot{q}_{\mathrm{rad}}$ and the radiation loses $\dot{q}_{\mathrm{rad}}$, where $\dot{q}_{\mathrm{rad}}$ is the radiative heating rate. The balanced entropy budget of the steady climate and the radiation is described by the two following equations (Weiss 1996; Goody 2000), respectively:

$$\int_V \left(\frac{\dot{q}_{\mathrm{rad}}}{T} + \dot{s}_{\mathrm{mat}}\right)\rho dV = 0, \quad \text{climate} \tag{1}$$

$$\int_{\mathrm{TOA}} \dot{\mathbf{s}}_{\mathrm{pl}} \cdot \mathbf{n} dA = \int_V \left(\frac{-\dot{q}_{\mathrm{rad}}}{T} + \dot{s}^{\mathrm{irr}}_{\mathrm{rad}}\right)\rho dV, \quad \text{radiation} \tag{2}$$

where the volume integrals are over the whole volume V of the climate system and the surface integral in (2) over the top of the atmosphere (TOA), $\mathbf{n}$ is the normal unit vector defined on TOA, $\dot{\mathbf{s}}_{\mathrm{pl}}$ the (upward) entropy flux at TOA. For convenience, we list the most important symbols we use in Table 1, and abbreviations in Table 2. Note that lower-case $\dot{s}$ and $\dot{q}$ are intensive quantities, while upper-case $\dot{S}$ and $\dot{Q}$ are extensive.

Equation 1 is the entropy budget equation for the matter and it states that in a steady state climate the radiative entropy source $\dot{S}^{\mathrm{rev}}_{\mathrm{rad}} = \int(\dot{q}_{\mathrm{rad}}/T)\rho dV$, where T is the temperature at which the energy is gained or lost, must be balanced by the rate of *material* entropy production $\dot{S}_{\mathrm{mat}}$ due to material irreversible processes: viscous and thermal dissipation, latent and sensible heating, etc.

In a steady state the entropy of the climate system is not changing, so the net radiative entropy flux at the top of the atmosphere $\dot{S}_{\mathrm{pl}} = \int_{\mathrm{TOA}} \dot{\mathbf{s}}_{\mathrm{pl}} \cdot \mathbf{n} dA$ must equal the *planetary* entropy production. Equation 2 describes the entropy budget for the radiation interacting with the climate system. It says that the planetary entropy production in a steady state is equal to the sum of the radiative entropy sink of the matter $-\dot{S}^{\mathrm{rev}}_{\mathrm{rad}} = \int(-\dot{q}_{\mathrm{rad}}/T)\rho dV$, which Goody (2000) calls *reversible* (since the heat is transferred from the radiation to the matter through a series of local equilibrium states which are by definition locally reversible), and the *irreversible* entropy production $\dot{S}^{\mathrm{irr}}_{\mathrm{rad}} = \int dV \dot{s}^{\mathrm{irr}}_{\mathrm{rad}}$ due to thermalization of the absorbed and emitted photons (Goody and Abdou 1996). The processes which contribute to $\dot{S}^{\mathrm{irr}}_{\mathrm{rad}}$ are discussed in Ozawa et al. (2003) and Fraedrich and Lunkeit (2008) and Sect. 4.

By adding (1) and (2) we obtain:

$$\int_{\mathrm{TOA}} \dot{\mathbf{s}}_{\mathrm{pl}} \cdot \mathbf{n} dA = \int_V \left(\dot{s}_{\mathrm{mat}} + \dot{s}^{\mathrm{irr}}_{\mathrm{rad}}\right)\rho dV \tag{3}$$

which now gives us a joint description of matter and radiation in the Earth system. Equation 3 states that the total entropy carried out of the Earth system by electromagnetic radiation

Table 1 List of symbols

Symbol	Description	Units
$\dot{q}_k$	Specific heating rate due to process k	W kg^{-1}
$\dot{Q}_k$	Global integral of heating due to process k	W
$\dot{s}_k$	Specific entropy source due to process k	W kg^{-1} K^{-1}
$\dot{S}_k$	Global integral entropy source due to process k	W K^{-1}
$\dot{S}$	Global integral rate of change of entropy of the climate system	W K^{-1}
$\dot{S}_{\mathrm{mat}}$	Global integral rate of material entropy production	W K^{-1}
$\dot{\mathbf{s}}_{\mathrm{pl}}$	Outgoing entropy flux at TOA	W m^{-2} K^{-1}
$\dot{s}^{\mathrm{irr}}_{\mathrm{rad}}$	Specific rate of radiative irreversible entropy production	W kg^{-1} K^{-1}
$\tau_{x,y}$	Zonal and meridional component of the turbulent stresses	N m^{-2}
H	Sensible heat flux at the surface, positive upwards	W m^{-2}
$\mathcal{L}$	Latent heat flux at the surface, positive upwards	W m^{-2}
ε	Specific dissipation rate of kinetic energy	W kg^{-1}
D	Global integral dissipation rate of kinetic energy	W
θ_L	Liquid-frozen potential temperature	K
q	Specific humidity	g kg^{-1}
$q_{L/F}$	Liquid/frozen cloud water	g kg^{-1}
L_z	Longwave radiative flux at level z	W m^{-2}
e_z	Longwave emission at level z	W m^{-2}
$\mathcal{T}_z$	Transmittivity at level z	–

Table 2 List of abbreviations used in the text

Abbreviations	Description
"adv"	Advection
"at"	Atmosphere
"bl"	Boundary layer
"conv"	Convection
"diff"	Temperature diffusion
"diss"	Dissipation
"encor"	Energy correction
"hor"	Horizontal diffusion
"ice"	Ice physics
"irr"	Irreversible
"lh"	Latent heat
"solid"	Solid Earth and cryosphere
"ls"	Large scale precipitation
"lw"	Longwave
"mat"	Matter
"ml"	Ocean mixed-layer mixing
"oc"	Ocean
"pl"	Planetary
"rad"	Radiation
"sh"	Sensible heat
"sur"	Surface
"sw"	Shortwave
"TOA"	Top of the atmosphere
"tur"	Turbulent
"ver"	Vertical diffusion

equals the sum of the *material* entropy production $\dot{S}_{\mathrm{mat}}$ and the irreversible source of radiative entropy production $\dot{S}^{\mathrm{irr}}_{\mathrm{rad}}$ taking place inside the Earth system

$$\dot{S}_{\mathrm{pl}} = \dot{S}_{\mathrm{mat}} + \dot{S}^{\mathrm{irr}}_{\mathrm{rad}} = -\dot{S}^{\mathrm{rev}}_{\mathrm{rad}} + \dot{S}^{\mathrm{irr}}_{\mathrm{rad}}. \quad (4)$$

3.2 Method for diagnosis of entropy sources

In non-equilibrium thermodynamics (Kondepudi and Prigogine 1998) the specific material entropy production, i.e. not including radiation, has the form:

$$\dot{s}_{\mathrm{mat}} = \epsilon/T + \mathbf{F}\cdot\nabla(1/T) - \mathbf{J}_i\cdot\nabla(\mu_i/T), \quad (5)$$

where $\mathbf{F}$ is the material heat flux, $\mathbf{J}_i$ the diffusive mass flux of the ith chemical species, with chemical potential μ_i, and ε the specific dissipation rate of kinetic energy due to viscous forces. We omit the contribution from chemical reactions. The first term can be diagnosed directly in a GCM (Sect. 6). The second term is hard to deal with because in a GCM $\mathbf{F}$ is not represented by processes transporting heat down a temperature gradient; many parametrised processes are typically involved, which do not involve fluxes and gradients explicitly. On the other hand, local heating rates are quite easily diagnosed for these processes. A heating rate can be written in terms of the convergence of $\mathbf{F}$ and, from elementary calculus,

$$\int_V (-\nabla\cdot\mathbf{F})/T dV = \int_V \mathbf{F}\cdot\nabla(1/T)dV - \int_A (\mathbf{F}/T)\cdot\mathbf{n}dA \quad (6)$$

over a volume V with boundary A. If we integrate over the whole climate system, by construction there is no boundary term, because heat fluxes through the boundary are purely radiative, not material. Hence, when the whole climate system is taken into account, the *entropy production rate* due to **F** (first on the right) equals the volume integral of the *entropy source* (on the left).

In the present work, following Fraedrich and Lunkeit (2008), the climate entropy sources/sinks are computed "directly" based on temperature and temperature tendencies. In this method the entropy source associated with the physical process k is calculated from the local diabatic heating $\dot{q}_k$ according to:

$$\dot{s}_k = \frac{\dot{q}_k}{T}, \quad (\mathrm{WK^{-1}kg^{-1}}), \tag{7}$$

i.e. in terms of the temperature increments:

$$\dot{s}_k = c_p \frac{1}{T}\frac{\partial T_k}{\partial t} \simeq c_p \frac{1}{T}\frac{\Delta T_k}{\Delta t}, \tag{8}$$

where t is time, c_p the specific heat capacity at constant pressure, ΔT_k the temperature increment after the process k and Δt the physics timestep. In the model timestep the temperature is incremented sequentially after each process. In the present study T is chosen to be the temperature after the process. In the limit of small timesteps the processes are simultaneous and T is uniquely defined. Since the entropy source is due to a local convergence or divergence of heat, it can be positive or negative, unlike entropy production, which is due to processes that transport heat but cause zero net heating, and which is positive definite according to the second law of thermodynamics.

To express the heating rates and the entropy sources in W m^{-2} and W $m^{-2}K^{-1}$ we have to multiply (8) by the mass per unit area between the upper and lower vertical boundaries of the grid-box. Because the model makes the hydrostatic approximation, the required factor is $(-\Delta p/g)$, where Δp is the pressure difference between the upper and lower vertical boundaries of the grid-box.

In the ocean we have available from the model output the potential temperature θ and the potential temperature increments due to the different parametrisation schemes, $d\theta_k/dt$ for process k. By using the general relation between potential temperature θ and entropy s (Vallis 2006), $ds = c_p(p_R, \theta)d\theta/\theta$, and noting that in HadCM3 $c_p(p_R, \theta) = \tilde{c}$ is constant, we can diagnose the entropy source using the following equation:

$$\dot{s}_k \simeq \tilde{c}\frac{1}{\theta}\frac{\Delta\theta_k}{\Delta t}. \tag{9}$$

The third term on the right of Eq. 5 accounts for changes of phase of water, molecular diffusion of water vapour, etc., by direct calculation involving chemical potentials. The global integral of this term can be evaluated instead from the rate at which heat is added (removed) to (from) the hydrological cycle, that is from the latent heating associated with evaporation at the surface and phase changes within the atmosphere and from the temperatures at which this occurs. This gives the net entropy production by the hydrological cycle indirectly (Kleidon 2009).

3.3 Material entropy production by the climate system

In terms of material sources (7–9) the global integral rate of material entropy production is written:

$$\dot{S}_{\mathrm{mat}} = \sum_k \sum_c \int_{V_c} \rho dV \frac{\dot{q}_k^c}{T}, \quad (\mathrm{WK^{-1}}) \tag{10}$$

where the sum over c refers to the subsystems of the climate system, i.e. the atmosphere, the ocean, and the solid Earth and cryosphere, which we denote together as "solid". T is the local temperature in each subsystem where the heat $\dot{q}_k^c$ is released, k are the non-radiative diabatic processes, and the integrals are extended over the volume of the climate subsystems V_c.

Let us write (10) in terms of the quantities available from the model in order to identify them. The heating rates considered are those due to viscous dissipation and material heat transport, including latent heating. In the model, viscous dissipation in the atmosphere $\epsilon = \dot{q}^{\mathrm{at}}_{\mathrm{diss}}$, but viscous dissipation is neglected in the ocean, and is absent in the solid Earth. Atmosphere model processes cause sensible and latent heating $\dot{q}^{\mathrm{at}}_{\mathrm{sh}}, \dot{q}^{\mathrm{at}}_{\mathrm{lh}}$ within the body of the atmosphere and $\dot{q}^{\mathrm{oc,\,solid}}_{\mathrm{sh}}, \dot{q}^{\mathrm{oc,\,solid}}_{\mathrm{lh}}$ in the surface layer of the ocean and solid Earth. Within the ocean model, there are heating rates due to turbulent mixing processes (diffusion and mixed layer physics) $\dot{q}^{\mathrm{oc}}_{\mathrm{tur}}$. We neglect the entropy production due to the heat conduction within the ground which has been estimated by Weiss (1996) and Kleidon (2009) to be about 1 mW m^{-2} K^{-1}

Hence (10) can be expanded as:

$$\begin{aligned}\dot{S}_{\mathrm{mat}} = &\int_{V_{\mathrm{at}}} \frac{\dot{q}^{\mathrm{at}}_{\mathrm{diss}}}{T}\rho dV + \int_{V_{\mathrm{at}}} \frac{\dot{q}^{\mathrm{at}}_{\mathrm{lh}} + \dot{q}^{\mathrm{at}}_{\mathrm{sh}}}{T}\rho dV \\ &+ \int_{V_{\mathrm{solid}}} \frac{\dot{q}^{\mathrm{solid}}_{\mathrm{lh}} + \dot{q}^{\mathrm{solid}}_{\mathrm{sh}}}{T}\rho dV + \int_{V_{\mathrm{oc}}} \frac{\dot{q}^{\mathrm{oc}}_{\mathrm{lh}} + \dot{q}^{\mathrm{oc}}_{\mathrm{sh}}}{T}\rho dV + \int_{V_{\mathrm{oc}}} \frac{\dot{q}^{\mathrm{oc}}_{\mathrm{tur}}}{T}\rho dV,\end{aligned} \tag{11}$$

where V_{at}, V_{oc}, V_{solid} are the volumes of the atmosphere, ocean and solid Earth. Because $\dot{q}^{\mathrm{solid}}_{\mathrm{sh}}, \dot{q}^{\mathrm{solid}}_{\mathrm{lh}}, \dot{q}^{\mathrm{oc}}_{\mathrm{sh}}, \dot{q}^{\mathrm{oc}}_{\mathrm{lh}}$ exist only in the surface layer of the solid Earth and ocean, we can rewrite them:

$$\int_{V_{\text{solid}}} \frac{\dot{q}_{\text{sh}}^{\text{solid}} + \dot{q}_{\text{lh}}^{\text{solid}}}{T} \rho dV = -\int_{A_{\text{land}}} dA \frac{H^{\text{solid}} + \mathcal{L}^{\text{solid}}}{T_{\text{sur}}}, \tag{12}$$

$$\int_{V_{\text{oc}}} \frac{\dot{q}_{\text{sh}}^{\text{oc}} + \dot{q}_{\text{lh}}^{\text{oc}}}{T} \rho dV = -\int_{A_{\text{oc}}} dA \frac{H^{\text{oc}} + \mathcal{L}^{\text{oc}}}{T_{\text{sur}}} \tag{13}$$

where T_{sur} is the surface temperature, H and $\mathcal{L}$ are the sensible and latent heat flux respectively (positive upwards, so these fluxes cool the surface), and A_{oc} and A_{land} are the ocean and land surfaces. The latent and sensible heat fluxes are available from the model, so these terms can be readily evaluated. Noting that $A_{\text{oc}} \cup A_{\text{land}} = A$, i.e. the whole interface between the atmosphere and the land–ocean, (11) can be further rewritten:

$$\dot{S}_{\text{mat}} = \int_{V_{\text{at}}} \frac{\dot{q}_{\text{diss}}^{\text{at}}}{T} \rho dV + \left(\int_{V_{\text{at}}} \frac{\dot{q}_{\text{sh}}^{\text{at}}}{T} \rho dV - \int_{\text{A}} dA \frac{H}{T_{\text{sur}}} \right) + \left(\int_{V_{\text{at}}} \frac{\dot{q}_{\text{lh}}^{\text{at}}}{T} \rho dV - \int_{\text{A}} dA \frac{\mathcal{L}}{T_{\text{sur}}} \right) + \int_{V_{\text{oc}}} dV \frac{\dot{q}_{\text{tur}}^{\text{oc}}}{T} \rho dV. \tag{14}$$

By defining

$$\dot{S}_{\text{diss}} \equiv \int_{V_{\text{a}}} \frac{\dot{q}_{\text{diss}}^{\text{at}}}{T} \rho dV, \tag{15}$$

$$\dot{S}_{\text{sh+lh}} \equiv \dot{S}_{\text{sh+lh}}^{\text{at}} + \dot{S}_{\text{sh+lh}}^{\text{sur}} \tag{16}$$

$$\dot{S}_{\text{sh+lh}}^{\text{at}} \equiv \int_{V_{\text{a}}} \frac{\dot{q}_{\text{lh}}^{\text{at}} + \dot{q}_{\text{sh}}^{\text{at}}}{T} \rho dV, \quad \dot{S}_{\text{sh+lh}}^{\text{sur}} \equiv -\int_{A_{\text{sur}}} dA \frac{H + \mathcal{L}}{T_{\text{sur}}}, \tag{17}$$

$$\dot{S}_{\text{tur}}^{\text{oc}} \equiv \int_{V_{\text{oc}}} \frac{\dot{q}_{\text{tur}}^{\text{oc}}}{T} \rho dV, \tag{18}$$

we summarise Eq. 14 thus:

$$\dot{S}_{\text{mat}} = \dot{S}_{\text{diss}} + \dot{S}_{\text{sh+lh}} + \dot{S}_{\text{tur}}^{\text{oc}}. \tag{19}$$

To this we may add two unphysical sources of entropy from the atmosphere model: $\dot{S}_{\text{diff}}$ due to temperature hyperdiffusion, which is included for numerical stability, and $\dot{S}_{\text{adv}}$ due to inaccuracy in the advection by the dynamical core.

In Table 4 the vertically integrated global averages are shown of the entropy sources and diabatic heatings described in the following sections.

When radiative heating rates are also included in a formula like (10) we obtain the rate of change of entropy $\dot{S}$ of the climate system:

$$\dot{S} = \sum_c \int_{V_{\text{c}}} \rho dV \left(\sum_k \frac{\dot{q}_{\text{k}}^{\text{c}}}{T} + \frac{\dot{q}_{\text{rad}}^{\text{c}}}{T} \right). \tag{20}$$

Now (20) can be easily identified as the integrand function in (1), which states that $\dot{S} = \dot{S}_{\text{rad}}^{\text{rev}} + \dot{S}_{\text{mat}} = 0$, i.e. the rate of change of entropy of the climate system is zero in a steady state. This holds also for any subsystem of the climate separately, e.g. the atmosphere.

4 Radiative entropy production within the climate system

4.1 The radiation scheme

The atmosphere comprises N emitting-absorbing levels ($N = 19$ in HadCM3 and $N = 11$ in FAMOUS). The radiation scheme consists of two parts, solar (shortwave) and thermal (longwave) (Edwards and Slingo 1996), using six shortwave bands and eight longwave bands. It includes the effects of greenhouse gases: CO_2, H_2O, O_3, O_2, N_2O, CH_4, CFC11 and CFC12. The calculations of the radiative fluxes within the atmosphere allow an estimate of the shortwave heating rate $\dot{q}_{\text{sw}}$ and the longwave heating rate $\dot{q}_{\text{lw}}$. From these last we obtain $\dot{s}_{\text{rad}}^{\text{rev}} = \dot{q}_{\text{sw}}/T + \dot{q}_{\text{lw}}/T$ (Eqs. 1, 2). The radiation generates a large entropy sink (~ -390 mW m^{-2} K^{-1}) in the body of the atmosphere because it is dominated by longwave cooling, the atmosphere being heated mainly non-radiatively from the surface by latent and sensible heat.

4.2 The irreversible radiative entropy production

As pointed out by Weiss (1996) and Goody (2000) the irreversible radiative entropy production $\dot{S}_{\text{rad}}^{\text{irr}}$ is a large term compared with the *material* entropy production $\dot{S}_{\text{mat}}$ and thus it dominates the planetary entropy production $\dot{S}_{\text{pl}}$ (see Table 3). The radiative processes accounted for by $\dot{S}_{\text{rad}}^{\text{irr}}$ are the thermalization of absorbed shortwave radiation $\dot{S}_{\text{sw}}^{\text{irr}}$ and the absorption and reemission of longwave radiation $\dot{S}_{\text{lw}}^{\text{irr}}$ within the climate system. Thermalization is the process in which the molecules after the absorption of photons rearrange their energy levels towards lower energy modes. This is a small-scale process whereby local thermodynamic equilibrium is maintained; when considering the climate entropy budget, we are concerned with larger scales, and local thermodynamic equilibrium is assumed always to apply. The large irreversible radiative entropy production is not relevant to the operation of the material climate system, as can be understood by a thought experiment, in which we imagine there is no radiation, but instead we provide the climate system at every point with heat sources and sinks equal to shortwave absorption and net longwave emission. This substitution of a different mechanism for external energy exchange would not affect the evolution of the

Table 3 The global integral entropy budget obtained from HadCM3 and FAMOUS is compared with other GCM simulations and observations

Process	HadCM3	FAMOUS	Fraedrich and Lunkeit (2008)	Goody (GISS)	Goody	Peixoto
Radiative entropy terms						
$\dot{S}_{\mathrm{pl}}$	911.3	897.8	882	–	–	892
$\dot{S}_{\mathrm{sw}}^{\mathrm{irr}}$	811.8	790.9	812	802	–	819
$\dot{S}_{\mathrm{lw}}^{\mathrm{sur,at}}$	10.6	10.2	6	–	–	24
$\dot{S}_{\mathrm{lw}}^{\mathrm{at,at}}$	38.6	42.7	28	–	–	–
$\dot{S}_{\mathrm{rad}}^{\mathrm{irr}}$	861.0	843.7	846	–	–	843
$\dot{S}_{\mathrm{rad}}^{\mathrm{rev}}$	−51.0	−54.1	–	−72.8	–	–
Material entropy terms						
$\dot{S}_{\mathrm{sh+lh}}$	37.8	37.9	29	58.7	21.2	25
$\dot{S}_{\mathrm{sh}}^{\mathrm{bl}}$	2.2	2.3	1	3.4	2.4	2.1
$\dot{S}_{\mathrm{diss}}$	12.5[a]	13.6[a]	6[b]	11.5	11.3	7
$\dot{S}_{\mathrm{diff}}$	0.8	1.1	–	–	–	–
$\dot{S}_{\mathrm{adv}}$	−0.1	−0.4	–	–	–	–
$\dot{S}_{\mathrm{tur}}^{\mathrm{oc}}$	0.8	1.0	–	–	–	–
$\dot{S}_{\mathrm{mat}}$	51.8	53.3	35	70.2	32.5	34.1
Rate of change of entropy						
$\dot{S}$	0.8	−0.8	−7	−2.6	–	−17

In the table here both material and radiative terms discussed in Sects. 3–8 are summarized. All the terms are in mW m^{-2} K^{-1}

[a] The term denoted by "diss" is from the energy correction in HadCM3 and FAMOUS

[b] The estimate in Fraedrich and Lunkeit (2008) is deduced from the total entropy imbalance

Some values from Peixoto et al. (1991) have been updated after Kleidon and Lorenz (2005). The value of $\dot{S}_{\mathrm{sw}}^{\mathrm{irr}}$ in Goody has been calculated from values given in Table 6 in Goody (2000) assuming $T_{\mathrm{Sun}} = 5{,}777$ K. Values of $\dot{S}_{\mathrm{tur}}^{\mathrm{oc}}$ are here averaged over the whole surface and therefore different from the ones shown in Table 6

climate system, since the fluid equations are concerned only with the amount of heat gained or lost. Nonetheless, we calculate $\dot{S}_{\mathrm{rad}}^{\mathrm{irr}}$, following Ozawa et al. (2003), Peixoto et al. (1991) and Fraedrich and Lunkeit (2008). We also calculate $\dot{S}_{\mathrm{pl}}$ from the incoming shortwave and outgoing longwave radiation; the entropy flux carried by a radiation beam is obtained by dividing the flux of radiative energy by the emission temperature.

4.3 The shortwave radiation

Let us first consider the solar shortwave radiation. In the radiation scheme the solar radiation is represented as a vertically orientated downward beam which is partly absorbed at every level and finally at the surface. We will not consider the entropy associated with scattering and reflection. If we assume the brightness temperature of the incoming radiation to be that of the surface of sun, $T_{\mathrm{Sun}} = 5.777$ K, the *incoming* entropy flux $\dot{S}_{\mathrm{sw}}^{\mathrm{pl}} = F_{\mathrm{sw}}^{\mathrm{TOA}}/T_{\mathrm{Sun}}$ (noting that the net $\dot{S}_{\mathrm{pl}}$ is defined as positive *outwards*), where $F_{\mathrm{sw}}^{\mathrm{TOA}}$ is the net downward shortwave radiative flux at the TOA. This flux is absorbed within the climate system, such that $F_{\mathrm{sw}}^{\mathrm{TOA}} = \int dA \int \rho dz \dot{q}_{\mathrm{sw}} + \int dA F_{\mathrm{sw}}^{\mathrm{sur}}$, where $F_{\mathrm{sw}}^{\mathrm{sur}}$ is the net downward flux at the surface. Then from Eq. 4 we have

$$\dot{S}_{\mathrm{sw}}^{\mathrm{irr}} = \int dA \int dz \dot{q}_{\mathrm{sw}} \left(\frac{1}{T} - \frac{1}{T_{\mathrm{Sun}}} \right) + \int dA F_{\mathrm{sw}}^{\mathrm{sur}} \left(\frac{1}{T_{\mathrm{sur}}} - \frac{1}{T_{\mathrm{Sun}}} \right). \tag{21}$$

The first term is associated with the absorption of light in the atmosphere and the second accounts for absorption at the surface. Equation 21 is formally identical to Eqs. 16a, 16b in Ozawa et al. (2003) but allows for a differential absorption throughout the atmosphere.

4.4 The longwave radiation

Longwave irreversible entropy production $\dot{s}_{\mathrm{lw}}^{\mathrm{irr}}$ is calculated as the sum of two components: emission–absorption longwave interaction within the atmosphere, $\dot{s}_{\mathrm{lw}}^{\mathrm{at,at}}$, and emission–absorption longwave interaction between the surface and the atmosphere, $\dot{s}_{\mathrm{lw}}^{\mathrm{sur,at}}$.

Exact calculation of the $\dot{s}_{\mathrm{lw}}^{\mathrm{at,at}}$ and $\dot{s}_{\mathrm{lw}}^{\mathrm{sur,at}}$ would require the knowledge of the transmittivity and emissivity at every frequency ν. Here we have decided to provide a first approximation for $\dot{S}_{\mathrm{lw}}^{\mathrm{irr}}$ based on spectrally integrated radiative transfer. In the radiation scheme it is easy to obtain the upward and downward longwave fluxes at every model half level (interfaces between model layers), say $L_{z+1/2}(\uparrow)$ and $L_{z+1/2}(\downarrow)$. By neglecting the spectral dependence for

transmittivity $\mathcal{T}(\nu)$ and assuming the emissivity to be $1-\mathcal{T}$, we can express the fluxes at each half-level as

$$\begin{aligned} L_{z+1/2}(\uparrow) &= e_z + \mathcal{T}_z L_{z-1/2}(\uparrow), \\ L_{z-1/2}(\downarrow) &= e_z + \mathcal{T}_z L_{z+1/2}(\downarrow) \end{aligned} \tag{22}$$

from which we can obtain the following estimates for $\mathcal{T}_z$ and the Plank sources e_z at every model level z:

$$\mathcal{T}_z = \frac{L_{z+1/2}(\uparrow) - L_{z-1/2}(\downarrow)}{L_{z-1/2}(\uparrow) - L_{z+1/2}(\downarrow)}, \quad e_z = L_{z+1/2}(\uparrow) - \mathcal{T}_z L_{z-1/2}(\uparrow). \tag{23}$$

$\dot{s}_{\mathrm{lw}}^{\mathrm{at,at}}$ is determined by the longwave interaction of any two atmospheric layers i and j at temperature T_i and T_j. The layer i emits an energy amount e_i via longwave radiation, which crosses the intermediate layers through which it is partially transmitted arriving at layer j, where a fraction $(1-\mathcal{T}_j)$ is absorbed. The same happens for the emission e_j partially absorbed at the level i. Hence $\dot{S}_{\mathrm{lw}}^{\mathrm{at,at}}$ can be written as:

$$\dot{S}_{\mathrm{lw}}^{\mathrm{at,at}} = \sum_{i=1}^{N} \sum_{j>i} \mathcal{C}_{ij} \left(\frac{1}{T_j} - \frac{1}{T_i} \right) \tag{24}$$

where the coefficients $\mathcal{C}_{ij}$ are given by:

$$\mathcal{C}_{ij} = \begin{cases} \left[e_i(1-\mathcal{T}_j) - e_j(1-\mathcal{T}_i) \right] \prod_{l=i+1}^{j-1} \mathcal{T}_l & j-i>1 \\ e_i(1-\mathcal{T}_j) - e_j(1-\mathcal{T}_i) & j-i=1. \end{cases}$$

The estimate of $\dot{S}_{\mathrm{lw}}^{\mathrm{sur,at}}$ (Eq. 16c) in Ozawa et al.(2003) requires knowledge of the upwelling longwave radiation emitted by the surface (say e_{sur}) and partially absorbed at the level i and conversely of the radiation e_i emitted at the level i and absorbed at the surface. This term can be written as:

$$\dot{S}_{\mathrm{lw}}^{\mathrm{sur,at}} = \sum_{i=1}^{N} \mathcal{G}_i \left(\frac{1}{T_i} - \frac{1}{T_{\mathrm{sur}}} \right) \tag{25}$$

where the coefficients $\mathcal{G}_i$ are:

$$\mathcal{G}_i = \begin{cases} e_{\mathrm{sur}}(1-\mathcal{T}_1) - e_i & i=1 \\ e_{\mathrm{sur}}[(1-\mathcal{T}_i) - e_i] \prod_{l=1}^{i-1} \mathcal{T}_l & i>1. \end{cases}$$

4.5 The planetary entropy production

The planetary entropy production is the difference between the outgoing planetary longwave entropy flux $\dot{S}_{\mathrm{lw}}^{\mathrm{pl}}$ and the incoming solar shortwave entropy flux $\dot{S}_{\mathrm{sw}}^{\mathrm{pl}} = F_{\mathrm{sw}}^{\mathrm{TOA}}/T_{\mathrm{Sun}}$ at the top of the atmosphere. In order to estimate the longwave entropy flux the longwave energy flux at the top of the atmosphere $F_{\mathrm{lw}}^{\mathrm{TOA}}$ must be decomposed into its emission level components:

$$F_{\mathrm{lw}}^{\mathrm{TOA}} = \Lambda_{\mathrm{sur}} + \sum_{z=1}^{N} \Lambda_z, \tag{26}$$

where Λ_{sur} is the longwave radiation originated at the ground reaching the top of the atmosphere, which in our approximation is:

$$\Lambda_{\mathrm{sur}} = e_{\mathrm{sur}} \mathcal{T}_1 \mathcal{T}_2, \ldots, \mathcal{T}_N \tag{27}$$

and Λ_z the longwave flux emitted at the atmospheric model level z and still reaching the top of the atmosphere:

$$\Lambda_z = e_z \mathcal{T}_{z+1} \mathcal{T}_{z+2}, \ldots, \mathcal{T}_N. \tag{28}$$

Emissions e_z and transmittivities $\mathcal{T}_z$ are calculated as shown in (23).

The approximation (22) is quite good. This can be checked comparing the value of $F_{\mathrm{lw}}^{\mathrm{TOA}}$ obtained from the functions (27), (28) with the one available in the model diagnostics in which the radiative transfers are properly calculated. The two fields are very similar indeed. Despite the crudeness of the approximation (22) it is surprising to see that typical differences at TOA are 0.4 W m^{-2} or less in FAMOUS (i.e. a relative error of about 0.2%) and 0.02 in HadCM3 ($\sim$0.01%). More significant differences are on the polar regions and on the South Pole particularly though, where our approximation leads to underestimates of up to $\sim$2%.

Thus the planetary entropy production is:

$$\dot{S}_{\mathrm{pl}} = \dot{S}_{\mathrm{pl}}^{\mathrm{lw}} - \dot{S}_{\mathrm{pl}}^{\mathrm{sw}} = \frac{\Lambda_{\mathrm{sur}}}{T_{\mathrm{sur}}} + \sum_{z=1}^{N} \frac{\Lambda_z}{T_z} - \frac{F_{\mathrm{sw}}^{\mathrm{TOA}}}{T_{\mathrm{Sun}}}, \tag{29}$$

which is formally identical to Eq. 12 in Ozawa et al. (2003).

We estimate the error in the longwave entropy flux as $\Delta\dot{S}_{\mathrm{pl}} \sim \Delta L/T$, where ΔL is a typical mean value for the flux error and T a typical temperature. Taking $\Delta L \sim 0.2$ W m^{-2} from the model output and $T \sim 270$ K we have $\Delta\dot{S}_{\mathrm{pl}} \sim 0.7$mW m^{-2}K^{-1}, which is quite small if compared to the typical values of $\dot{S}_{\mathrm{pl}} \sim 900$ mW m^{-2}K^{-1} (see Table 3). This estimate of the error is of the same order of magnitude of the residual in the balance Eq. 2 we found in the model (1.2 W m^{-2} K^{-1} in HadCM3 and 0.2 W m^{-2}K^{-1} in FAMOUS), as can be seen in Table 3.

5 Sensible and latent heating

5.1 Convection

The convection incorporates several irreversible processes which lead to diabatic heating $\dot{q}_{\mathrm{conv}}$ and an entropy source $\dot{s}_{\mathrm{conv}}$. Water vapour condensation of the saturated rising parcels releases a considerable amount of heat in the surrounding cloud environment. At the same time the rising parcel interacts with the "external" environment through entrainment and detrainment at the edges of the cloud.

In the convection scheme all these processes are implemented in the convective cloud model, and lead to an increment of the cloud potential temperature. After updating the cloud properties, the scheme finds out the impact on the environment, i.e. on the model primary variables θ and q. In fact, as usual in all mass flux schemes, the plume interacts with its environment through en/detrainment of heat, moisture and cloud liquid water and subsidence induced in the cloud environment which compensates for the parcel's upward mass flux. The expressions for the net change of environmental potential temperature and specific humidity are quite involved and can be found in Gregory and Rowntree (1990), Eqs. (21a, b).

By looking at Table 4 and Figs. 1b, 2b we note that the entropy source associated with the convection scheme is the largest non-radiative term, and is concentrated mainly in the upper tropical atmosphere.

5.2 The large-scale cloud and precipitation scheme

The large scale cloud scheme (Smith 1990) operates diagnostically using the values of the so-called "cloud-conserved variables" to calculate the new cloud amount in every grid box and the new amounts of water vapour, liquid and frozen cloud water. These variables are the total water content $q_t = q + q_L + q_F$ (where q is the water vapour and q_L and q_F the liquid and frozen water contents, respectively) and the liquid-frozen water potential temperature $\theta_L = \theta - (L_C/c_p)q_L - \{(L_C + L_F)/c_p\}q_F$ (where L_C and L_F are the latent heat of condensation and fusion respectively and c_p the specific heat capacity at constant pressure). θ_L and q_t are not affected by changes of phase, and nor is the corresponding liquid-frozen temperature $T_L = T - (L_C/c_p)q_L - \{(L_C + L_F)/c_p\ \}q_F)$, while q_L and q_F are incremented by amounts dq_L, dq_F. As a consequence a net temperature increment dT is implied:

$$dT = \frac{L_C}{c_p} dq_L + \frac{L_C + L_F}{c_p} dq_F. \tag{30}$$

This air temperature change is due to latent heat $c_p\ dT$ associated with condensation/evaporation forced by the dynamics and all the physical processes which "unbalance" the cloud, i.e. which make it inconsistent with the required diagnostic relations.

The large scale precipitation scheme (Gregory 1995) deals with micro-physical processes associated with large scale precipitation: evaporation of rain and sublimation of frozen precipitation in sub-saturated regions, freezing and melting of the cloud water if this is in an inappropriate state before it is converted to liquid or frozen precipitation. The temperature increments contribute to the total large scale cloud diabatic heating $\dot{q}_{\rm ls}$ and to the entropy source $\dot{s}_{\rm ls}$, which peaks in the mid-latitude regions (see Fig. 1c).

5.3 Boundary layer

The boundary layer scheme (Smith 1990) determines the transport processes of momentum, latent heat and sensible heat in the lowest atmospheric levels and at the surface (the boundary layer levels are five in HadCM3 and three in FAMOUS). The boundary layer heating term $\dot{q}_{\rm bl}$ and entropy source $\dot{s}_{\rm bl}$ are the sum of two contributions: one due to the divergence of sensible heat (enthalpy) fluxes and the other due to condensation of some moisture forced by the vertical turbulent motions leading to the formation of low clouds. The scheme is implemented by using the cloud conserved temperature T_L and hence "T_L fluxes" $F_{T\_L} = \rho\langle w'\ \dot{T_L}\rangle$ are used on the boundary layer levels to work out T_L increments (here we have used the usual formalism of fluctuations and averaging of the statistical theory of the turbulence). The relation between the temperature increment dT and dT_L is, from the T_L definition:

$$dT = dT_L + \frac{L_C}{c_p} dq_L + \frac{L_C + L_F}{c_p} dq_F. \tag{31}$$

From dT we calculate the boundary layer entropy source (Figs. 1d, 2d), which is quite intense but of course confined to the lower troposphere.

Table 4 List of the area-averaged vertically integrated entropy sources/sinks and diabatic heatings for the atmosphere and the surface for a 50 year control run in FAMOUS and HadCM3

	Atmosphere								Ocean and solid		
	$\dot{S}^{\rm rev}_{\rm rad}$	$\dot{S}_{\rm conv}$	$\dot{S}_{\rm ls}$	$\dot{S}_{\rm bl}$	$\dot{S}_{\rm diff}$	$\dot{S}_{\rm encor}$	$\dot{S}_{\rm adv}$	Total	$\dot{S}^{sur}_{\rm sh+lh}$	$\dot{S}^{\rm rev}_{\rm rad}$	Total
HadCM3	−392.1	235.3	69.9	73.1	0.8	12.5	−0.1	−0.7	−340.5	341.1	0.6
FAMOUS	−397.6	265.4	44.4	72.2	1.1	13.6	−0.4	−1.2	−344.1	343.8	−0.3
	$\dot{Q}_{\rm rad}$	$\dot{Q}_{\rm conv}$	$\dot{Q}_{\rm ls}$	$\dot{Q}_{\rm bl}$	$\dot{Q}_{\rm diff}$	$\dot{Q}_{\rm encor}$	–	Total	$H + \mathcal{L}$	$\dot{Q}_{\rm rad}$	Total
HadCM3	−101.9	63.3	17.5	21.1	0.1	3.1	–	3.2	−101.2	101.7	0.5
FAMOUS	−103.1	71.6	10.5	20.9	0.1	3.4	–	3.5	−103.1	102.5	0.6

The different terms are associated to the different parametrisation schemes discussed in Sect. 4–7. There is no heating associated with the numerical entropy sinks. The entropy sources are expressed in mW $m^{-2}K^{-1}$ and the heating rates in W m^{-2}

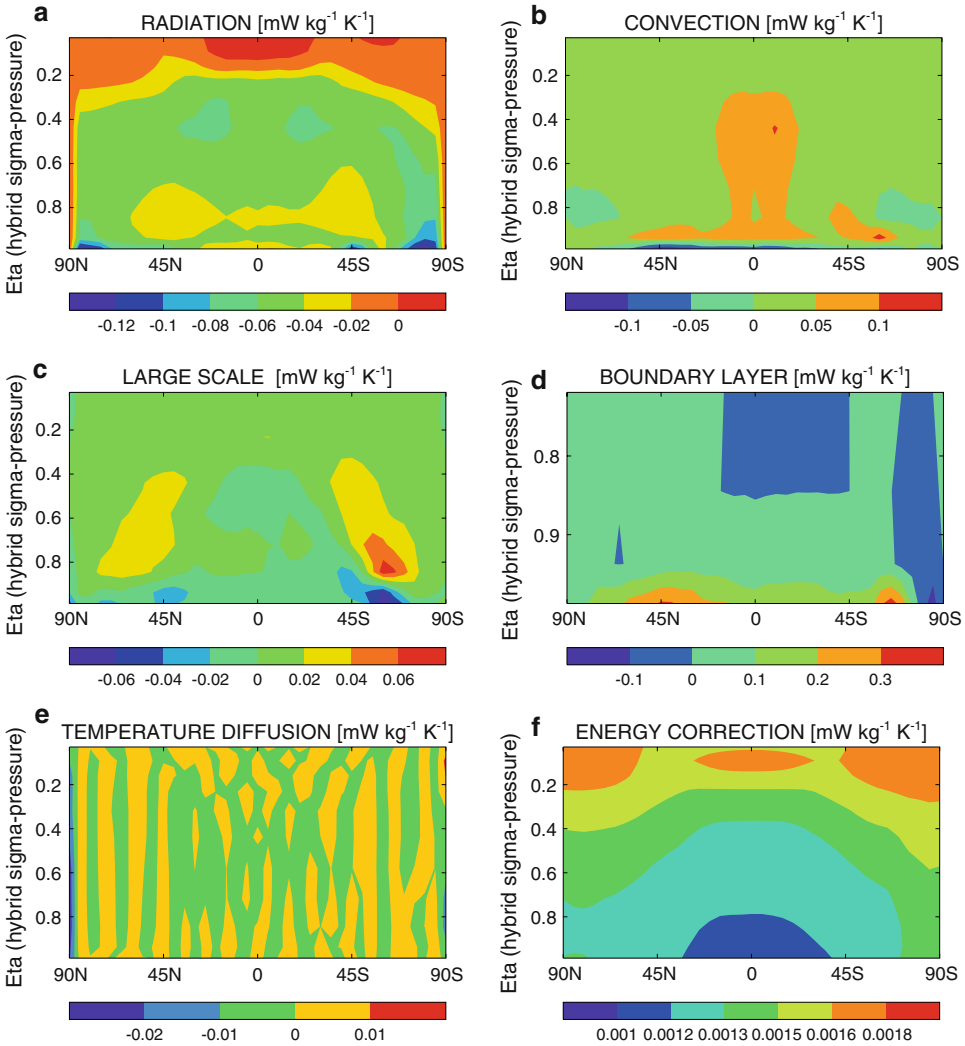

Fig. 1 Fifty year zonal means of the specific entropy sources $\dot{s}_{\rm rad}, \dot{s}_{\rm conv}, \dot{s}_{\rm ls}, \dot{s}_{\rm bl}, \dot{s}_{\rm diff}$ and $\dot{s}_{\rm encor}$(mW kg^{-1}K^{-1}) within the atmosphere from FAMOUS

It is not known how much of dq_L and dq_F is due to condensation and how much simply to convergence of the q_L and q_F fluxes. In order to know that we would need to know those fluxes, but the scheme just uses the fluxes of q_t. Hence it is not possible to separate uniquely the two different contributions to $\dot{s}_{\rm bl}$ from sensible heat and condensation. The cloud scheme case is different in this respect because no flux divergences are present and thus changes in q_L and q_F are entirely due to local water vapour condensation into cloud water. In other words the HadCM3 boundary layer scheme is intrinsically ignorant about the partitioning of sensible and latent heating. This is an example of the shortcomings of models that are not generally constructed to deal with an accurate treatment of entropy.

An approximate estimate of the entropy produced by the vertical turbulent fluxes of sensible heat within the boundary layer can be obtained when we recall that at the surface (which coincides with the first boundary layer level in the model), $F^*_{T\_L} = H$, because at the surface $q_L = q_F = 0$, i.e. there is no surface flux of cloud water, only water vapour. Furthermore, we know that $F_{T\_L} = F_T = 0$ above the boundary layer levels. Therefore the convergence of the vertical turbulent fluxes of sensible heat must take place completely within the boundary layer. A very simple approximation is:

$$\dot{S}^{\rm bl}_{\rm sh} \simeq \int_{\rm sur} H\left(\frac{1}{\tilde{T}} - \frac{1}{T_{\rm sur}}\right) dA, \tag{32}$$

where $\tilde{T}$ is a temperature representative of the boundary layer convergence of the sensible heat flux. We have arbitrarily chosen the temperature on the second model half-level (the first half level is the surface) corresponding to a pressure level of approximately 950 hPa since the convergence of F_{T_L} takes place mostly between the surface and the first model levels. Within this approximation, we can see from Table 3 that the entropy production due to the hydrological cycle is $\sim$35.6 mW m^{-2}K^{-1}, that is $\dot{S}_{\rm sh+lh} - \dot{S}^{\rm bl}_{sh}$.

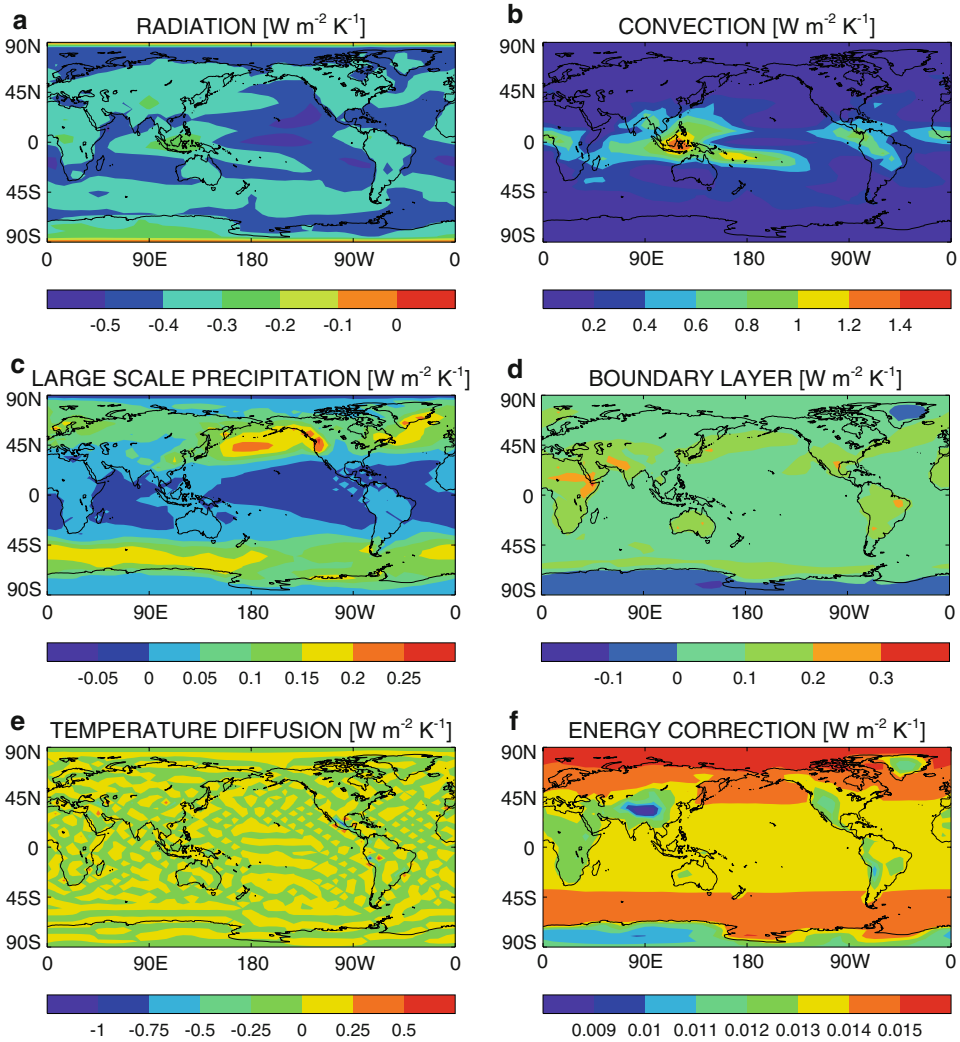

Fig. 2 Fifty year mean of the mass weighted vertical integrals of the entropy sources $\dot{s}_{\rm rad}, \dot{s}_{\rm conv}, \dot{s}_{\rm ls}, \dot{s}_{\rm bl}, \dot{s}_{\rm diff}$ and $\dot{s}_{\rm encor}$ (W m^{-2}K^{-1}) from FAMOUS

5.4 Temperature hyper-diffusion

The temperature hyper-diffusion terms $\dot{q}_{\rm diff}$ and $\dot{s}_{\rm diff}$ have a characteristic vertically striped pattern due to the numerics of the diffusion operator. This is quite unphysical as it can be observed in Figs. 1e, 2e. The hyper-diffusion term has almost no effect on the overall heating ($\sim$0.09 W m^{-2}) but although no net heat is added to the atmosphere, the heat is moved down a temperature gradient which generates entropy of around 1 mW m^{-2}K^{-1}.

6 The energy correction and the dissipation of kinetic energy

6.1 The meaning of the energy correction in HadCM3

The atmosphere energy correction (Gregory 1998) is introduced in the model to account for the energy loss after every timestep. This loss is diagnosed by comparing the change in the atmosphere total kinetic and moist static energy over each timestep with the convergence of surface and TOA heat fluxes. The imbalance is ascribed to the neglect by the atmosphere model of the heating D due to kinetic energy dissipation by the internal stresses, i.e.

$$\mathcal{E} = D = \int_V dV \tau : \nabla \mathbf{v} \tag{33}$$

where τ is the stress tensor. $\mathcal{E}$ is converted into a temperature increment $dT = \mathcal{E}/(c_p M), M$ being the mass of the atmosphere, which is applied uniformly to the temperature field in the model. The cross section of the associated specific entropy source is shown in Fig. 1f, where it can be noted that it is inversely proportional to the temperature field (since when expressed in mW kg^{-1}K^{-1}, $\dot{s}_{\rm encor} \propto dT/T$) whereas in Fig. 2f the mass weighted vertical integral of $\dot{s}_{\rm encor}$ shows the proportionality to the mass of the atmospheric vertical column.

We can check that the energy correction $\mathcal{E}$ effectively corresponds to the total amount of dissipated kinetic energy by calculating the change in the total

(thermal + gravitational) potential energy $P = \int(c_v\ T + gz)\rho dV$ during the advection step in the model. In fact from the energy cycle formalism (Peixoto and Oort 1992) the links between dissipation $D = \int \rho\varepsilon\ dV$, kinetic energy $K = \int \rho dV\ (\mathbf{v}\cdot\mathbf{v})/2$, the rate of conversion of potential energy into kinetic energy $C(P, K) = -\int dV\ \mathbf{v}\cdot\nabla p$, the total diabatic heating $\dot{Q}$ and P are:

$$\dot{K} = -D + C(P, K) \tag{34}$$

$$\dot{P} = -C(P, K) + \dot{Q} \tag{35}$$

which says that in a steady state ($\dot{K} = \dot{P} = 0$) the dissipation must be equal to the rate at which potential energy is converted into kinetic energy ($D = C$) and that $\dot{Q} = D$. Now let us divide the atmospheric timestep of the model into an advective step, during which the equations are integrated and no diabatic heating is added, and a following physics step, when the diabatic heating is added up by all the physics schemes. This division is unphysical but it reflects the way the model works. Hence all the quantities involved can written as the sum of an "advective" part and a "physics" part, e.g. $\dot{P} = \dot{P}_{\text{adv}} + \dot{P}_{\text{phy}}$, where $\dot{P}_{\text{adv}}$ is the rate of change of P during the advective step and $\dot{P}_{\text{phy}}$ during the physics step. During the advection in the model there is no diabatic heating, $\dot{Q} = 0$, hence $-\dot{P}_{\text{adv}} = C_{\text{adv}}$. We note that $C(P, K) = 0$ during the physics step since there is no conversion of potential energy into kinetic (during the physics step kinetic energy, and thus the horizontal wind (u, v), is altered only by the viscous drag and this term is accounted in D; apart from this the wind is unaffected). It follows that $-\dot{P}_{\text{adv}} = \dot{P}_{\text{phy}} = \dot{Q} = D$. Therefore in a steady state model climate the dissipation rate must be equal to minus the variation of total potential energy during the advective step. We estimate $\dot{P}_{\text{adv}}$ using the Lorenz formula $P = \int c_p\ T\ \rho dV$, which is valid for an atmosphere over a flat surface. This is not the case for HadCM3 but here we are not interested in a very precise estimate of P but just in corroborating the interpretation of the energy correction as dissipation.

In Fig. 3a, b the time series of $\mathcal{E}$ and $-\dot{P}_{\text{adv}}$ are plotted showing that despite a constant bias of less than 0.1 W m^{-2} the curves are substantially the same. The bias might be attributed to numerical inaccuracy or the small imbalance in the diabatic heating (0.1 W m^{-2}, see Table 4).

6.2 The dissipative processes in the model

In the model there are four explicit processes causing the dissipation of the specific kinetic energy $(\mathbf{v}\cdot\mathbf{v})/2$: (a) the turbulent eddy stresses in the boundary layer scheme associated with the vertical diffusion of horizontal momentum; (b) the hyper-diffusion term in the momentum equation for (u, v); (c) the gravity wave drag and (d) the impact on the large scale flow due to the convective eddy-flux stresses. Of course in reality the mechanical dissipation of kinetic energy takes place only at the very small scales of the molecular viscosity (millimetres or less) towards which it is drained down by the turbulent energy cascade. But in a GCM we do not resolve such small scales and therefore we have to parametrize it by using phenomenological expressions for the eddy-stresses.

The total amount of viscous dissipation $D = \int_{V\_\text{at}} \rho\varepsilon\ dV$ due to the eddy-stresses is given by the mass integral over the entire atmospheric volume of the specific kinetic energy tendency $\partial_t(\mathbf{v}^2/2) = \mathbf{v}\cdot\partial_t\mathbf{v}$ caused by them. This can be readily seen if we write the hydrostatic kinetic energy equation:

$$d\frac{(\mathbf{v}^2/2)}{dt} = -\frac{1}{\rho}(\mathbf{v}\cdot\nabla_h p + \nabla\cdot\mathbf{F}_K) - \epsilon, \tag{36}$$

where $d/dt = \partial_t + \mathbf{v}\cdot\nabla_h$, ∇_h the horizontal gradient, τ the viscous stress tensor , $\mathbf{F}_K = \mathbf{v}\cdot\tau$, and $\varepsilon = \rho^{-1}\ \nabla_h\mathbf{v}\cdot\tau$ the local viscous dissipation. All advective and horizontal gradient terms are treated in the the dynamical core, so within the parametrizations (a–d) (36) is just $\partial_t(\mathbf{v}^2/2) = \rho^{-1}\nabla\cdot\mathbf{F}_K - \varepsilon$. If we integrate over the whole atmospheric volume and neglect the flux of kinetic energy into the ocean ($\sim$0.007 W m^{-2}, Peixoto and Oort 1992), we obtain $D = \int_{V\_\text{at}} \rho\varepsilon dV = \partial_t\int_{V\_\text{at}} \rho dV\ (\mathbf{v}^2/2)$. In the following, we describe how HadCM3 deals with the kinematic impact of the boundary layer, convection, gravity wave schemes and horizontal hyperdiffusion.

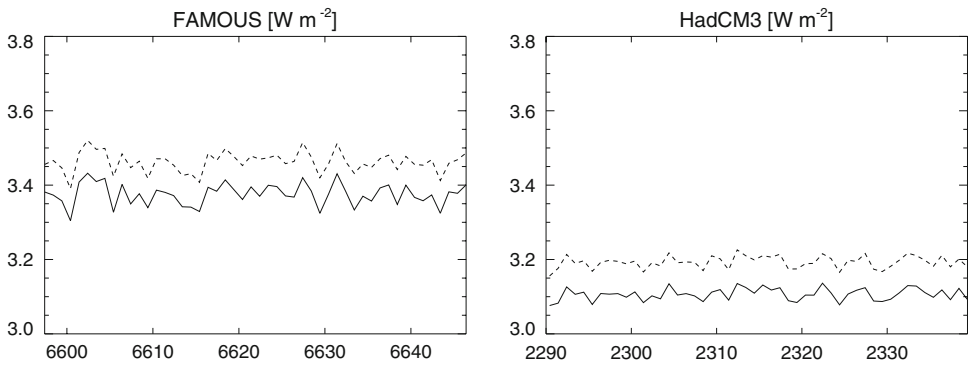

Fig. 3 Energy correction $\mathcal{E}$ (*continuous line*) and consumption of total potential energy $-\dot{P}_{\text{adv}}$ (*dashed line*) by atmospheric dynamics for FAMOUS and HadCM3

(a) *Turbulent stresses in the boundary layer: vertical momentum diffusion*. The vertical turbulent mixing of momentum affects the large scale circulation through the action of the eddy-stress $\tau^{bl} = \tau_x^{bl}\mathbf{i} + \tau_y^{bl}\mathbf{j}$ (Smith 1993). The model works out their impact on the horizontal flow according to:

$$\left(\frac{\partial \mathbf{v}}{\partial t}\right)_{bl} = -\frac{1}{\rho}\frac{\partial \tau^{bl}}{\partial z}. \tag{37}$$

(b) *Horizontal momentum diffusion*. A hyper-diffusion operator $\mathcal{D}$ is applied to horizontal velocity $\mathbf{v}$ yielding:

$$\left(\frac{\partial \mathbf{v}}{\partial t}\right)_{\text{hor}} = \mathcal{D}(\mathbf{v}), \tag{38}$$

$\mathcal{D}$ being a biharmonic operator of sixth order in HadCM3 and eight in FAMOUS (details in Cullen et al. 1993).

(c) *Gravity wave drag*. The drag of the mountains on the atmosphere is manifested in the production of gravity waves. The gravity wave drag scheme (Gregory et al. 1997b) determines the surface stress $\tau_{\text{sur}}^{\text{gw}}$ and the distribution of this stress through the atmospheric column τ^{gw}. Once the stresses are determined, the impact on the horizontal momentum is:

$$\left(\frac{\partial \mathbf{v}}{\partial t}\right)_{\text{gw}} = -\frac{1}{\rho}\frac{\partial \tau^{\text{gw}}}{\partial z}. \tag{39}$$

(d) *Convective momentum transport*. The mass-flux convection scheme implemented in the Unified Model (Gregory and Rowntree 1990) also accounts for the vertical mixing of horizontal momentum associated with convective updraughts and downdraughts. The effects of the subgrid-scale circulation upon the large-scale wind can be written as:

$$\left(\frac{\partial \mathbf{v}}{\partial t}\right)_{\text{conv}} = -\frac{\partial \overline{\mathbf{v}}'\omega'}{\partial p} \tag{40}$$

where $\omega = Dp/Dt$. The vertical eddy-flux of horizontal velocity can be expressed in terms of large-scale and cloud variables as (Gregory et al. 1997a) $\overline{\mathbf{v}'\omega'} = M_u(\mathbf{v}_u - \mathbf{v}) + M_d(\mathbf{v}_d - \mathbf{v})$, where M_u and $\mathbf{v}_u$ are the values of the cloud mass-flux and velocities in the updraught and M_d and $\mathbf{v}_d$ in the downdraught.

From (37–40) the kinetic energy tendencies and the dissipation terms are estimated and compared with the energy correction which is about 3.1 W m^{-2} in HadCM3 and 3.4 W m^{-2} in FAMOUS. The several dissipative contributions for the two models are shown in Table 5. Their sum is 3.0 W m^{-2} in HadCM3 and 3.2 W m^{-2} in FAMOUS and so a small residual still remains which has to be ascribed probably to filtering and the discretization error. It is found that about half of the dissipation is due to boundary layer stresses. The energy correction term in FAMOUS is slightly larger than in HadCM3 and the other terms are of comparable magnitude. Let us note though that the kinetic energy drain from the large scale flow (D_{bl}) is slightly higher in HadCM3 than in FAMOUS. The dissipation of kinetic energy due to the turbulent down-scale energy cascade generates an entropy source of $\sim$13 mW m^{-2} K^{-1}. For more discussion see Sect. 9.

Table 5 Area-averaged values for the vertically integrated dissipation rate of kinetic energy due to various processes in HadCM3 and FAMOUS

	$\mathcal{E}$	D_{bl}	D_{hor}	D_{conv}	D_{gw}	Residual
HadCM3	3.1	1.5	0.6	0.6	0.3	0.1
FAMOUS	3.4	1.4	0.8	0.8	0.2	0.2

All the values are W m^{-2}. The kinetic energy lost in the filtering is very small ($\sim$0.03 W m^{-2}) and hence not shown in the table above

7 Numerical entropy production in the dynamical core

In numerical models there is a small entropy source of a numerical nature (Johnson 1997; Egger 1999). Theoretically the advection is a perfectly adiabatic process. However in the numerical integration phenomena of pure numerical nature such as the numerical dispersion, Gibbs oscillation and numerical diffusion and filtering yield an entropy source. Moreover, the hyper-diffusion (Sect 5.4), required for the numerical stability and, de facto, part of the dynamic core, can be conceptually considered as part of the numerical entropy (Woollings and Thuburn 2006) although it is associated with an explicit heating. However this term, which is an unphysical one, may also be considered to represent the mixing of the small-scale eddies.

The numerical entropy produced by the advection scheme is not associated with a heating term. As a consequence we cannot apply (8) but it must be estimated as in Woollings and Thuburn (2006) using the more general relation between entropy s and potential temperature θ, $ds = c_p\,(d\theta/\theta)$ for a dry atmosphere. In our case if θ_a is the potential temperature after the advection timestep Δt and θ_b just before, the numerical entropy production during the timestep Δt is:

$$\dot{S}_{\text{adv}} = \left(\int_{V_{\text{at}}} \rho dV c_p \ln\theta_a - \int_{V_{\text{at}}} \rho dV c_p \ln\theta_b\right)/\Delta t. \tag{41}$$

We found in the control runs $\dot{S}_{\text{adv}} \sim -0.1$ mW m^{-2}K^{-1} (HadCM3) or ~ -0.4 mW m^{-2} K^{-1} (FAMOUS), which is the combined effect of adjustment, advection and Fourier filtering (Cullen and Davies 1991). Woollings and Thuburn (2006) found a term of similar magnitude but positive ($\sim$0.5 mW m^{-2}K^{-1}) using the Reading IGCM1 spectral

model (Hoskins and Simmons 1975). They considered the dynamical core as a whole, thus including also the effect of the hyper-diffusion in the computation of numerical entropy production. When we likewise sum $\dot{S}_{\mathrm{diff}} + \dot{S}_{\mathrm{adv}}$, we find numerical entropy sources of 0.7 mW $\mathrm{m}^{-2}\mathrm{K}^{-1}$ in HadCM3 and 0.6 mW $\mathrm{m}^{-2}\,\mathrm{K}^{-1}$ in FAMOUS, similar to IGCM1.

8 Entropy production in the ocean

The material entropy production in the ocean is due to three different processes: heat transport, viscous dissipation and molecular diffusion of salt ions. The last two are negligible and estimated to be one and two orders of magnitude smaller than that due to heat transport (Gregg 1984; Shimokawa and Ozawa 2001). Furthermore in HadCM3 ocean the dissipated kinetic energy is not accounted for at all in the energy equation. As a consequence we will consider only the entropy associated with diabatic heating in the model. Numerical entropy production is negligible in the ocean model.

8.1 Processes at the surface

Table 6 shows the area-averaged estimates of the vertically integrated sources and sinks of entropy in the ocean as simulated by HadCM3 and FAMOUS. It can be seen that the major part of the entropy is produced or destroyed at the top layers of the ocean model. The model divides these into three: the blue component of shortwave radiation, fluxes due to latent heating from sea-ice melting and freezing and snowfall into the ocean, and the net effect of all other atmosphere fluxes.

Table 6 List of ocean entropy sources and diabatic heatings for HadCM3 and FAMOUS

	$\dot{S}_{\mathrm{npen}}$	$\dot{S}_{\mathrm{pen}}$	$\dot{S}_{\mathrm{ice}}$	$\dot{S}_{\mathrm{ver}}$	$\dot{S}_{\mathrm{hor}}$	$\dot{S}_{\mathrm{ml}}$	Total
HadCM3	−290.2	294.6	−6.0	0.6	0.3	0.3	−0.4
FAMOUS	−291.1	296.5	−6.5	0.8	0.3	0.3	0.3
	$\dot{Q}_{\mathrm{npen}}$	$\dot{Q}_{\mathrm{pen}}$	$\dot{Q}_{\mathrm{ice}}$	$\dot{Q}_{\mathrm{ver}}$	$\dot{Q}_{\mathrm{hor}}$	$\dot{Q}_{\mathrm{ml}}$	Total
HadCM3	−85.3	86.8	−1.6	0	0	0	−0.1
FAMOUS	−85.8	87.8	−1.8	0	0	0	0.2

All the terms are averages over the ocean area of the vertically integrated specific entropies and heatings, units are mW $\mathrm{m}^{-2}\,\mathrm{K}^{-2}$ and W m^{-2}. The "npen" terms refer to the sum of longwave cooling, latent and sensible heat fluxes and shortwave radiation except the blue component, which is counted in the "pen" terms. The "ice" terms are for latent heating associated with sea-ice processes and snowfall into the ocean. The "ver" terms refer to vertical diffusion, "hor" to horizontal diffusion, "ml" to mixed-layer mixing and convection. Terms not shown in the table give heatings of less than 10^{-6} W m^{-2} and entropy sources of order 10^{-6} W $\mathrm{m}^{-2}\mathrm{K}^{-1}$ or less

8.2 Diffusion, mixing, convection, dynamics

Several irreversible processes are parametrised in the ocean model in order to reproduce the effects of the turbulence due to the sub-grid scale mixing: vertical diffusion, mixed layer physics, convective adjustment and isopycnal diffusion. From Table 6 we can see that these processes do not contribute to an overall heating of the ocean although locally they may be non-zero. That means that they just move heat from one point to another one inside the ocean without a flux contribution at the surface (a boundary flux). Conversely, they have a non-zero contribution to the ocean entropy budget since they move heat down a temperature gradient.

The dominant entropy source among the diabatic processes inside the ocean is $\dot{S}_{\mathrm{ver}}$ caused by the vertical diffusion of the potential temperature. This is the sum of two contributions: first, an explicit vertical diffusion, second the vertical component of the isopycnal diffusion. The explicit vertical diffusion is implemented as $\partial_z(\kappa(z)\partial_z\theta)$ where the vertical diffusion coefficient κ is the sum of a depth-dependent constant background term and a term dependent on the stability of the ocean and hence on the Richardson number as in Pacanowsky and Philander (1981).

Mixing in the ocean occurs predominantly along isopycnal surface, i.e. surfaces of equal density, which is why water masses tend to preserve their temperature and salinity characteristics over very large distances. In order to represent such a process a diffusion scheme which orients the mixing tensor along isopycnal surface is needed (Redi 1982). The isopycnal surfaces are mostly horizontal, particularly at the low-latitude regions, but in the high-latitude regions they can be quite steep. Therefore both a horizontal and a vertical component are present.

A further scheme implemented in the HadCM3 ocean model is Visbeck et al. (1997) version of the Gent and McWilliams (1990) scheme for the adiabatic thickness diffusion. This is a scheme introduced in order to parametrise the effects of mesoscale eddies on large scale density and tracer structures. This is achieved by mixing of isopycnal layer thickness along isopycnal surfaces and advecting tracers by the eddy-induced transport velocity derived from the isopycnal thickness mixing. As expected, since the scheme is intrinsically formulated to be adiabatic, its entropy contribution is insignificant.

The mixed layer scheme (Kraus and Turner 1967) works out a balance between the energy required for mixing the water column and the energy available as turbulent kinetic energy from the wind and from the introduction of buoyancy at the ocean surface, leading to convective instability. Water is mixed down from the surface to a level at which no more energy is available for mixing, producing a vertically homogeneous layer. The spatial pattern of the vertically integrated ocean entropy terms discussed in this section is shown in Fig. 4(a–f).

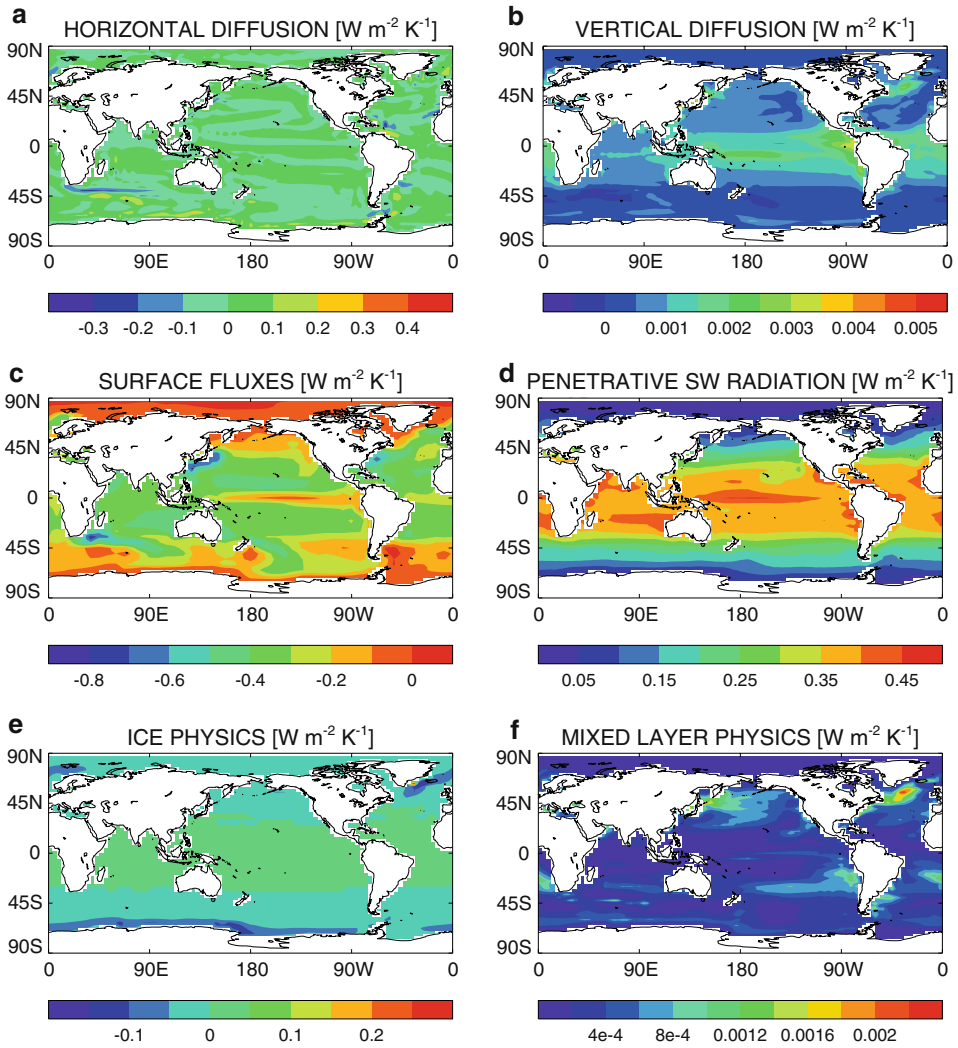

Fig. 4 Thirty years mean of the vertically integrated (W $m^{-2}K^{-1}$) entropy sources within the ocean: $\dot{s}_{hor}, \dot{s}_{ver}, \dot{s}_{sfc}, \dot{s}_{pen}, \dot{s}_{ice}, \dot{s}_{ml}$ from FAMOUS

The sum of the heat transport terms described in this section gives $\dot{q}^{oc}_{tur} = \dot{q}_{ver} + \dot{q}_{hor} + \dot{q}_{ml}$ and thus $\dot{S}^{oc}_{tur} = \dot{S}_{ver} + \dot{S}_{hor} + \dot{S}_{ml}$ (see Eq. 18), the material entropy production purely internal to the ocean. We obtain $\dot{S}^{oc}_{tur} = 1.2$ and 1.4 mW m^{-2} K^{-1} in HadCM3 and FAMOUS, averaged over the ocean surface only (0.8 and 1.0 mW $m^{-2}K^{-1}$ respectively when averaged over the whole Earth surface).

8.3 Comparison of estimates of ocean entropy production

Shimokawa and Ozawa (2001) used an idealised Atlantic Ocean with rectangular domain of 72° longitude by 140° latitude to diagnose the entropy productions due to heat transport, finding a value of about 2.5 mW $m^{-2}K^{-1}$, rather similar to our result for $\dot{S}^{oc}_{tur}$.

Yan et al. (2004) studied the entropy budget of the ocean using the energy fluxes and the temperature at the ocean surface. However they included $\dot{S}^{irr}_{rad}$ due to thermalization of shortwave radiation absorbed by the ocean (see Sect. 4.2), which dominates their estimated entropy production of 555.7 mW $m^{-2}K^{-1}$; typical values for $\dot{S}^{irr}_{rad}$ are $\sim$550 mW $m^{-2}K^{-1}$ (Kleidon and Lorenz 2005). Yan et al. (2004) do not provide any order-of-magnitude estimates for the material entropy production, which is hard to estimate from observations since it depends on the local gradients of temperature.

9 Climate entropy budget and the uncertainty in the material entropy production

The important issue we are dealing with in this paper is the entropy balance of the climate system. Obviously the climate, strictly, is never in a steady state but over a climatological period (decades) we can consider it to be, statistically speaking, in a steady state since we do not expect its properties to change substantially. General circulation models are usually built to be energetically balanced, e.g. to assure a null net radiative flux at the top of

the atmosphere, but not to be entropy balanced. Therefore it is an important question to check how well HadCM3 is entropy balanced and compare it with other models for which entropy diagnostics are available.

The complete climate entropy budget for HadCM3 and FAMOUS is shown in Table 3, where it is compared with estimates obtained from other models and theoretical computations (Fraedrich and Lunkeit 2008; Goody 2000; Peixoto et al. 1991).

The overall imbalance of the HadCM3 climate, i.e. $\dot{S}$ (see Sect.3), is shown in Table 3. In terms of the quantities listed in that table $\dot{S} = \dot{S}_{\rm rad}^{\rm rev} + \dot{S}_{\rm mat}$. HadCM3 has $\dot{S} \sim 0.8\,{\rm mW\ m^{-2}K^{-1}}$, which is quite small if compared with the typical fluctuations due to the interannual variability of most of the entropy terms which is of order 1 mW $\rm m^{-2}\,K^{-1}$. FAMOUS likewise has an entropy imbalance ~ -0.8 mW $\rm m^{-2}\,K^{-1}$ for the whole climate system, which is within the range of the interannual variability. The other two GCMs show a much higher imbalance as can be seen in Table 3.

There is greater planetary entropy production $\dot{S}_{\rm pl}$ in HadCM3 and FAMOUS than in the Planet Simulator of Fraedrich and Lunkeit (2008), who gave the only other value obtained from a GCM. However, at $\sim$900 mW $\rm m^{-2}\,K^{-1}$, both are close to the order-of-magnitude estimate by Peixoto et al. (1991). The next three rows are the irreversible entropy production terms of the radiative field as in Sect. 4.2. The shortwave absorption part is similar in HadCM3 and the Planet Simulator, while for FAMOUS we find a lower value. This difference is due mainly to differences in the shortwave fluxes in the two models, i.e. HadCM3 has a higher value of the shortwave energy radiation absorbed in the atmosphere than FAMOUS (283 vs. 266 W $\rm m^{-2}$). Also the difference in $\dot{S}_{\rm pl}$ is linked to different longwave flux at the top of the atmosphere (240 vs. 235 W $\rm m^{-2}$). The atmosphere–atmosphere longwave and surface–atmosphere longwave interaction is generally greater in the UM models ($\sim$50 vs. $\sim$34 mW $\rm m^{-2}\,K^{-1}$), which also has to be attributed to the differences in the model radiative properties.

In the remaining rows material entropy production terms can be seen. Unlike the radiative terms, the material terms are little affected by the differences in resolution between FAMOUS and HadCM3. Both UM models produce the same amount of entropy in the interaction of the solid Earth and ocean with the atmosphere through sensible and latent heating, $\dot{S}_{\rm sh+lh} \sim 38\,{\rm mW\,m^{-2}\,K^{-1}}$ (since both models have almost the same mean values of $H + \mathcal{L} \sim 102\,{\rm Wm^{-2}}$). More important differences can be noted though when a comparison is made with the other models. The HadCM3 value of $\dot{S}_{\rm sh+lh}$, mainly due to the hydrological cycle, is larger than the value found by Fraedrich and Lunkeit (2008) (29 mW $\rm m^{-2}\,K^{-1}$). This is not surprising since HadCM3 and the Planet Simulator differ substantially in the treatment of processes associated with water phase transitions. Phase changes of convective and large scale precipitation are not considered in the Planet Simulator while in HadCM3 these processes are dealt with; likewise in the Planet Simulator no storage of water in clouds is implemented and condensation occurs if the air is supersaturated, whereas HadCM3 has prognostic cloud water variables. $\dot{S}_{\rm sh+lh}$ is still larger than the order-of-magnitude estimate by Peixoto et al. (1991) (25 $\rm mWm^{-2}\,K^{-1}$) and Goody (2000) (21.2 mW $\rm m^{-2}\,K^{-1}$), but smaller than the one in Goody (2000) from the GISS model (59 mW $\rm m^{-2}\,K^{-1}$) where this term is dominated by moist and dry convection. Differences among GCM diagnostics can be understood in terms of differences in the ways the energy fluxes are represented in the models, e.g. the GISS model has a very large value for the sensible and latent heat fluxes, $H + \mathcal{L} \sim 120\,{\rm Wm^{-2}}$. The approximate estimate of $\dot{S}_{\rm sh}^{\rm bl}$ described in Sect. 5.3 is quite close to the one in Peixoto et al. (1991) and lies between those from the other GCMs. This highlights that the maximum uncertainity is associated with the entropy produced by the moist processes leading to latent heating, being the range $\sim$(20–36) mW $\rm m^{-2}\,K^{-1}$.

The dissipation term in the atmosphere is quite important and deserves some discussion. In Fraedrich and Lunkeit (2008) this term is not worked out directly because in the Planet Simulator the energy loss by friction is not transferred back by heating. This contribution is assumed to equal the entropy imbalance and estimated to be $\sim$6 mW $\rm m^{-2}\,K^{-1}$. However, other explanations are possible for an entropy imbalance; we would argue that it cannot be confidently attributed solely to this particular missing term.

Goody (2000) provides two estimates for the dissipative entropy production of about the same size. The first (11.5 mW $\rm m^{-2}\,K^{-1}$) is diagnosed in the GISS model and includes dissipation due to dry convection and surface drag (8.1 mW $\rm m^{-2}\,K^{-1}$), moist convection (2.7 mW $\rm m^{-2}\,K^{-1}$) and a stratospheric drag (0.7 mW $\rm m^{-2}\,K^{-1}$). In the dry convection term the contribution from the numerical drag term associated with the use of a binomial filter is included as well. The second estimate of 11.3 mW $\rm m^{-2}K^{-1}$ comes from a theoretical order-of-magnitude calculation in which typical values of the surface drag and velocities are taken into account. Goody estimates the entropy produced by stresses in the frictional boundary layer to be $\sim$6 mW $\rm m^{-2}\,K^{-1}$, due to dry convection in the free atmosphere to be around 4 mW $\rm m^{-2}\,K^{-1}$ and due to moist convection 1.3 mW $\rm m^{-2}\,K^{-1}$. The order-of-magnitude value provided by Peixoto et al. (1991) is 7 mW $\rm m^{-2}\,K^{-1}$, estimated from a diabatic frictional heating in the boundary layer of 1.9 W $\rm m^{-2}$ at a temperature of 280 K.

HadCM3 and FAMOUS have an entropy production due to the dissipation of kinetic energy which is higher than the

other model and observational estimates. The reason for that is the higher value of the dissipation rate $D \sim 3.1$ W m^{-2} discussed in Sect. 6 (see Table 5), which agrees with Goody (2000) but exceeds estimates from observations, e.g. ~ 1.9 W m^{-2} (Peixoto and Oort 1992), ~ 2.4W m^{-2} (Arpe et al. 1986) and other GCMs, e.g. ~ 2.0 W m^{-2} in NCAR community atmosphere model (Boville and Bretherton 2003). It is quite surprising how poor still is our knowledge of this fundamental thermodynamic quantity of the atmosphere and how different still are the estimates from most of the GCMs.

The sum of $\dot{S}_{\mathrm{sh+lh}}, \dot{S}_{\mathrm{diss}}, \dot{S}_{\mathrm{diff}}, \dot{S}_{\mathrm{adv}}$ and $\dot{S}^{\mathrm{oc}}_{\mathrm{tur}}$ is the material entropy production of the climate system, $\dot{S}_{\mathrm{mat}}$. In the HadCM3 simulation we found $\dot{S}_{\mathrm{mat}} = 51.8\,\mathrm{mW\ m^{-2}K^{-1}}$ and $\dot{S}_{\mathrm{mat}} = 53.3\,\mathrm{mW\ m^{-2}K^{-1}}$ in FAMOUS. These are intermediate between ~ 35 mW m^{-2}K^{-1} in Fraedrich and Lunkeit (2008) and ~ 70 mW m^{-2}K^{-1} in Goody (2000). As we have seen above, the part which is most model dependent is $\dot{S}_{\mathrm{sh+lh}}$, i.e. the hydrological cycle, and it is the one causing the wide spread. The uncertainity in the viscous dissipation term is less important, say [6−13] mW m^{-2}K^{-1}. The material entropy production has been argued to be an important diagnostic tool in the analysis and comparison of climate models (Kunz et al. 2008; Lucarini 2009; Lucarini et al. 2009), therefore a better knowledge of it from both observations and modelling would be valuable.

10 Conclusions

A detailed and comprehensive entropy budget analysis of a complex atmosphere–ocean general circulation model, HadCM3, and its low resolution version, FAMOUS, has been presented in this paper. This study represents the first case for an AOGCM, since previous ones were about a slab-model (Fraedrich and Lunkeit 2008) and an AGCM (Goody 2000).

The irreversible physics embedded in the model schemes yielding climate entropy sources has been accurately discussed and connected with the different kinds of entropy produced within the climate system, as well as the diagnostic methods to calculate the radiative entropy production and the material entropy production terms.

A perfectly entropy balanced model should have $\dot{S} = 0$ in ideal steady state conditions. We find that in HadCM3 $\dot{S} \sim 0.8\,\mathrm{mW\ m^{-2}K^{-1}}$ and in FAMOUS $\dot{S} \sim -0.8$ mW m^{-2} K^{-1} . The typical magnitude of entropy variations due to interannual variability is 1mW m^{-2} K^{-1}, hence HadCM3 and FAMOUS can be considered close to a steady state and quite well entropy balanced. In this respect either the model or the diagnostic techniques are better than the Planet Simulator ($\dot{S} \sim -7\,\mathrm{mW\ m^{-2}K^{-1}}$) and the GISS model ($\dot{S} \sim -3\,\mathrm{mW\ m^{-2}K^{-1}}$).

HadCM3 and FAMOUS are rather similar as far as entropy terms are concerned although the resolution is different. On the other hand, even though the results confirm to a certain extent the order-of-magnitude numbers obtained from (Goody 2000; Fraedrich and Lunkeit 2008), differences between HadCM3 and the other two models are much more substantial and this shows that the differences in the model formulation are very influential on the entropy budget.

The *material* entropy production is found to be around $\dot{S}_{\mathrm{mat}} \sim 50\,\mathrm{mW\ m^{-2}K^{-1}}$, and it is dominated by the latent heat transfer from the surface (i.e. ocean and land) to the atmosphere and within the atmosphere, $\sim 36\,\mathrm{mW\ m^{-2}K^{-1}}$, that is to say about 70% of the material entropy production. The next most important process is the atmospheric viscous dissipation $\dot{S}_{\mathrm{diss}} \sim 13\,\mathrm{mW\ m^{-2}K^{-1}}$, which accounts for nearly 25% of climate material entropy production. The remaining terms account for around the 3.5 % ($\dot{S}^{\mathrm{bl}}_{\mathrm{sh}}$) and 1 % ($\dot{S}^{\mathrm{oc}}_{\mathrm{tur}}, \dot{S}_{\mathrm{diff}}$). The study of the ocean reveals that whereas its contribution to $\dot{S}_{\mathrm{sh+lh}}$ is significant since most of the latent heat flux is concentrated over the oceans, the entropy due to the turbulent mixing within it is a very small contribution ($\dot{S}^{\mathrm{oc}}_{\mathrm{tur}} \sim 1\mathrm{mW\ m^{-2}K^{-1}}$) to the overall material entropy.

The numerical entropy produced by the atmosphere model dynamical core is even smaller, ~ 0.7 mW m^{-2}K^{-1} in both HadCM3 and FAMOUS, and it is the combined effect of the diffusion (positive) and the filtering-adjustment-advection (negative). This confirms the findings in Woollings and Thuburn (2006) who computed very similar values for a spectral dynamical core in isolation (0.5 mW m^{-2}K^{-1}).

Comparison with other estimates reveals substantial disagreement in the most important terms. By comparing $\dot{S}_{\mathrm{mat}}$ with the other estimates we see that HadCM3 estimate is intermediate within a range (30, 70) mW m^{-2} K^{-1} constrained by Goody (2000) and Fraedrich and Lunkeit (2008). The uncertainty is of almost 100%. Also a fundamental quantity, the total dissipation D, is quite poorly known from models and observations (range 1.9–3.6 W m^{-2}). All this suggests the need for future work to improve our knowledge of the basic thermodynamics of the climate system.

Acknowledgments Salvatore Pascale would like to thank Robert Plant for the help provided in the diagnostic coding. Jonathan Gregory was partly supported by the Joint DECC, Defra and MoD Integrated Climate Programme, DECC/Defra (GA01101), MoD (CBC/2B/0417_Annex C5). The authors also thank the two anonymous reviewers for their comments, which led to significant improvements on the original version of the manuscript.

References

Arpe K, Brankovic C, Oriol E, Speth P (1986) Variability in time and space of energetics from a long series of atmospheric data

produced by ECMWF. Beitraege zur Physik der Atmosphaere 59:321–355
Boville BA, Bretherton CS (2003) Heating and kinetic energy dissipation in the NCAR community atmosphere model. J Clim 16:3877–3887
Cox MD (1984) A primitive equation, three dimensional model of the ocean. GFDL ocean group technnical report no. 1, Princeton NJ, USA, 143 pp
Cullen M, Davies T (1991) A conservative split-explicit integration scheme with fourth order horizontal advection. Q J R Meteorol Soc 117:993–1002
Cullen M, Davies T, Mawson M (1993) Unified model documentation paper no. 10. Tech. rep., Meteorological Office, UK
DeGroot S, Mazur P (1984) Non-equilibrium thermodynamics. Kluwar, Dover
Edwards J, Slingo A (1996) Studies with a flexible new radiation code. Part I: Choosing a configuration for a large-scale model. Q J R Meteorol Soc 122:689–719
Egger J (1999) Numerical generation of entropies. Mon Weather Rev 127:2211–2216
Fraedrich K, Jansen H, Kirk E, Lunkeit F (2005) The planet simulator: towards a user friendly model. Meteorologische Zeitschrift 14:305–314
Fraedrich K, Lunkeit F (2008) Diagnosing the entropy budget of a climate model. Tellus A 60:921–931
Gent P, McWilliams J (1990) Isopycnal mixing in ocean circulations models. J Phys Oceanogr 20:150–155
Goody R (2000) Sources and sinks of climate entropy. Q J R Meteorol Soc 126:1953–1970
Goody R, Abdou W (1996) Reversible and irreversible sources of radiation entropy. Q J R Meteorol Soc 122:483–496
Gordon C, Cooper C, Senior C, Banks H, Gregory J, Johns T, Mitchell J, Wood RA (2000) The simulation of sst, sea ice extents and ocean heat transports in a version of the Hadley Centre coupled model without flux adjustments. Clim Dyn 16:147–168
Gregg MC (1984) Entropy generation in the ocean by small-scale mixing. J Phys Oceanogr 14:688–711
Gregory D (1995) A consistent treatment of the evaporation of rain and snow for use in large-scale models. Mon Weather Rev 123:2716–2732
Gregory D (1998) Unified model documentation paper no. 28. Tech. rep., Meteorological Office, UK
Gregory D, Rowntree P (1990) A mass flux convection scheme with representation of cloud ensemble characteristics and stability-dependent closure. Mon Weather Rev 118:1483–1506
Gregory D, Kershaw R, Innes P (1997a) Parametrization of momentum transport by convection. Part II: Tests in single-column and general circulation models. Q J R Meteorol Soc 123:1153–1183
Gregory D, Shutts GJ, Mitchell JR (1997b) A new gravity-wave-drag scheme incorporating anisotropic orography and low-level wave breaking: impact upon the climate of the UK Meteorological Office Unified Model. Q J R Meteorol Soc 124:463–493
Hoskins BJ, Simmons AJ (1975) A multi-layer spectral model and the semi-implicit method. Q J R Meteorol Soc 101:637–655
Johnson D (1997) "General coldness of climate" and the second law: implications for modelling the earth system. J Clim 10:2826–2846
Jones C, Gregory J, Thorpe R, Cox P, Murphy J, Sexton D, Valdes P (2005) Systematic optimisation and climate simulation of FAMOUS, a fast version of Had CM3. Clim Dyn 25:189–204
Kleidon A (2009) Nonequilibrium thermodynamics and maximum entropy production in the earth system. Naturwissenschaften 96:653–677
Kleidon A, Lorenz R (2005) Non-equilibrium thermodynamics and the production of entropy. Understanding complex systems. Springer, Berlin
Kleidon A, Schymansky S (2008) Thermodynamics and optimality of the water budget on land: a review. Geophys Res Lett 35:L20404
Kondepudi D, Prigogine I (1998) Modern thermodynamics: from heat engines to dissipative structure. Wiley, Hoboken
Kraus E, Turner J (1967) A one dimensional model of the seasonal thermocline. Part II. Tellus 19:98–105
Kunz T, Fraedrich K, Kirk E (2008) Optimisation of simplified GCMs using circulation indices and maximum entropy production. Clim Dyn 30:803–813
Lucarini V (2009) Thermodynamic efficiency and entropy production in the climate system. Phys Rev E 80:021118
Lucarini V, Fraedrich K, Lunkeit F (2009) Thermodynamic analysis of snowball earth hysteresis experiment: efficiency, entropy production and irreversibility. QJR Meterol Soc (in press)
Martyushev L, Seleznev V (2006) Maximum entropy production principle in physics, chemistry and biology. Phys Rep 426:1–45
Ozawa H, Ohmura A, Lorenz RD, Pujol T (2003) The second law of thermodynamics and the global climate system: a review of the maximum entropy production principle. Rev Geophys 41(4):1018. doi:10.1029/2002RG000113
Pacanowsky R, Philander G (1981) Parametrisation of vertical mixing in numerical models of the tropical oceans. J Phys Oceanogr 11:1443–1451
Paltridge GW (1975) Global dynamics and climate—a system of minimum entropy exchange. Q J R Meteorol Soc 101:475–484
Pauluis O, Held M (2002) Entropy budget of an atmosphere in radiative–convective equilibrium. Part I: Maximum work and frictional dissipation. J Atmos Sci 59:125–139
Peixoto J, Oort A, de Almeida M, Tomé A (1991) Entropy budget of the atmosphere. J Geophys Res 96:10981–10988
Peixoto JP, Oort AH (1984) Physics of climate. Rev Mod Phys 56:365–429
Peixoto JP, Oort A (1992) Physics of the climate. Springer, New York
Pope VD, Gallani ML, Rowntree PR, Stratton RA (2000) The impact of new physical parametrizations in the Hadley Centre climate model—HadAM3. Clim Dyn 16:123–146
Redi M (1982) Oceanic isopycnal mixing by coordinate rotation. J Phys Oceanogr 12:1154–1158
Reichler T, Kim J (2008) How well do coupled models simulate today's climate? Bull Am Meteorol Soc 89:303–311
Shimokawa S, Ozawa H (2001) On the thermodynamics of the oceanic general circulation: entropy increase rate of an open dissipative system and its surroundings. Tellus 53A:266–277
Smith R (1990) A scheme for predicting layer clouds and their water content in a general circulation model. Q J R Meteorol Soc 116:435–460
Smith R (1993) Unified model documentation paper no. 24. Tech. rep., Meteorological Office, UK
Smith RS, Gregory JM, Osprey A (2008) A description of the FAMOUS (version xdbua) climate model and control run. Geosci Mod Dev 1:147–185
Vallis GK (2006) Atmospheric and oceanic fluid dynamics. Cambridge University Press, Cambridge
Visbeck M, Marshall J, Haine T, Spall M (1997) On the specification of eddy transfer coefficients in coarse resolution ocean circulation models. J Phys Oceanogr 27:381–402
Weiss W (1996) The balance of entropy on earth. Contin Mech Thermodyn 8:37–51
Woollings T, Thuburn J (2006) Entropy sources in a dynamical core atmosphere model. Q J R Meteorol Soc 132:43–59
Yan Y, Gan Z, Qi Y (2004) Entropy budget of the ocean system. Geophys Res Lett 30:L14311